

Cab45S inhibits the ER stress-induced IRE1-JNK pathway and apoptosis via GRP78/BiP

L Chen^{1,3}, S Xu^{1,3}, L Liu¹, X Wen¹, Y Xu¹, J Chen^{*,1,2} and J Teng^{*,1}

Disturbance of endoplasmic reticulum (ER) homeostasis causes ER stress and leads to activation of the unfolded protein response, which reduces the stress and promotes cell survival at the early stage of stress, or triggers cell death and apoptosis when homeostasis is not restored under prolonged ER stress. Here, we report that Cab45S, a member of the CREC family, inhibits ER stress-induced apoptosis. Depletion of Cab45S increases inositol-requiring kinase 1 (IRE1) activity, thus producing more spliced forms of X-box-binding protein 1 mRNA at the early stage of stress and leads to phosphorylation of c-Jun N-terminal kinase, which finally induces apoptosis. Furthermore, we find that Cab45S specifically interacts with 78-kDa glucose-regulated protein/immunoglobulin heavy chain binding protein (GRP78/BiP) on its nucleotide-binding domain. Cab45S enhances GRP78/BiP protein level and stabilizes the interaction of GRP78/BiP with IRE1 to inhibit ER stress-induced IRE1 activation and apoptosis. Together, Cab45S, a novel regulator of GRP78/BiP, suppresses ER stress-induced IRE1 activation and apoptosis by binding to and elevating GRP78/BiP, and has a role in the inhibition of ER stress-induced apoptosis.

Cell Death and Disease (2014) 5, e1219; doi:10.1038/cddis.2014.193; published online 8 May 2014

Subject Category: Cancer

The endoplasmic reticulum (ER) is an essential organelle for multiple cellular functions such as maintaining calcium homeostasis and the biosynthesis of proteins or lipids.^{1,2} Perturbation of the ER environment, such as disturbance of redox homeostasis, aberrations in calcium regulation, glucose deprivation and viral infection, can cause ER stress and trigger a response termed the unfolded protein response (UPR), which ensures that only properly folded proteins are sent to the plasma membrane or secreted.³ UPR signaling activation is mediated by three ER membrane transducers, PRKR-like ER kinase (PERK), activating transcription factor 6 and inositol-requiring kinase 1 (IRE1), and reduces ER stress by inhibiting protein transcription, expanding the ER membrane and elevating chaperon levels that enhance protein-folding ability in the ER.⁴ However, under severe or prolonged ER stress where ER homeostasis cannot be restored, the UPR triggers apoptosis, which is mainly mediated by PERK and IRE1 signaling.⁵ PERK activation leads to the phosphorylation of eIF2 α and selectively induces ATF4, a transcription factor that enhances the expression of pro-apoptotic CCAAT/enhancer-binding protein homologous protein (CHOP).⁶ IRE1 activation has dual functions in apoptosis. It can splice X-box-binding protein 1 (XBP1) mRNA to promote cell survival.⁷ However, during severe ER stress conditions, IRE1 recruits

TNF receptor-associated factor 2 and apoptosis signal-regulating kinase 1, then activates c-Jun N-terminal kinase (JNK) and induces apoptosis.^{8,9} A recent study also showed that under ER stress conditions, IRE1 splices certain microRNAs that inhibit caspase-2 expression and thus induces apoptosis.¹⁰

The 78-kDa glucose-regulated protein (GRP78), also known as immunoglobulin heavy-chain binding protein (BiP), is a chaperon protein belonging to the HSP70 family and predominantly resides in the lumen of the ER. GRP78/BiP, as a vital regulator of ER function, has critical roles in facilitating protein folding and assembly, protein transport, calcium homeostasis and regulating ER transmembrane transducers.^{11–13} In various pathological conditions, especially in growing tumors with a hypoxic environment, GRP78/BiP is strongly induced, inhibiting cancer cell apoptosis and promoting tumor growth.^{14,15} It forms a complex with BIK, a BH3-only protein, which is mainly distributed in the ER membrane and inhibits breast cancer cell apoptosis induced by estrogen starvation.¹⁶ GRP78/BiP also interacts with the sigma-1 receptor on the mitochondrion-associated ER membrane to regulate ER-mitochondria Ca²⁺ and cell survival.¹⁷ In certain types of tumors, highly expressed GRP78/BiP partially translocates to the plasma membrane where it interacts with

¹Key Laboratory of Cell Proliferation and Differentiation of the Ministry of Education, State Key Laboratory of Bio-membrane and Membrane Bio-engineering, College of Life Sciences, Peking University, Beijing, China and ²Center for Quantitative Biology, Peking University, Beijing, China

*Corresponding author: J Chen or J Teng, Key Laboratory of Cell Proliferation and Differentiation of the Ministry of Education, State Key Laboratory of Bio-membrane and Membrane Bio-engineering, College of Life Sciences, Peking University, 5 Yiheyuan Road, Beijing 100871, China. Tel/Fax: +86 10 62755786; E-mail: chenjg@pku.edu.cn (JC) or Tel: +86 10 62767044; Fax: +86 10 62755786; E-mail: junlnteng@pku.edu.cn (JT)

³These authors contributed equally to this work.

Keywords: Cab45S; GRP78/BiP; IRE1; ER stress; UPR; apoptosis

Abbreviations: CHOP, CCAAT/enhancer-binding protein homologous protein; ER, endoplasmic reticulum; ERdj4, ER-localized DnaJ 4/microvascular differentiation gene 1; GRP78/BiP, 78-kDa glucose-regulated protein/immunoglobulin heavy chain binding protein; IRE1, inositol-requiring kinase 1; JNK, c-Jun N-terminal kinase; NBD, nucleotide-binding domain; p-IRE1, phosphorylated IRE1; PERK, PRKR-like ER kinase; TUNEL, terminal deoxynucleotidyl transferase dUTP nick end labeling; UPR, unfolded protein response; XBP1, X-box-binding protein 1; XBP1s, spliced XBP1

Received 20.1.14; revised 19.3.14; accepted 1.4.14; Edited by H-U Simon

prostate apoptosis response-4 to regulate extrinsic apoptotic pathways¹⁸ or forms a complex with cripto to promote tumor cell growth.^{19,20} However, the precise regulatory mechanisms controlling the expression levels and functions of GRP78/BiP remain unclear.

Cab45, encoded by the *SDF4* gene, contains three isoforms: Cab45S, Cab45G and Cab45C, and belongs to the CREC protein family, which is mainly distributed in the secretory pathway.²¹ Cab45G influences Ca^{2+} entry into the trans-Golgi network where it regulates cargo sorting, whereas Cab45C regulates amylase exocytosis process by interacting with SNARE proteins in the cytoplasm.²² A proteome study showed that the Cab45S protein level was upregulated more than 20-fold in a pancreatic cancer cell line secretome,²³ but its functions remained largely unknown. Therefore, we designed experiments to determine the roles of Cab45S in cancer cell apoptosis and found that Cab45S regulates the activation of the

IRE-JNK signal pathway via GRP78/BiP, and has an important role in inhibiting ER stress-induced apoptosis.

Results

Cab45S inhibits ER stress-induced apoptosis. To investigate the function of Cab45S in ER stress-induced apoptosis, we first determined the effect of Cab45S on cell survival after treatment with the ER stress-inducing drugs thapsigargin (TG) and tunicamycin (TM). The viability of HeLa cells was assessed by cell proliferation assay (MTS assay) and the results showed that overexpression of 3 × Flag-Cab45S resulted in the survival of more cells after TG or TM treatment of different drug concentrations or different periods (Figure 1a, $P=1.64 \times 10^{-2}$ and Figure 1b, $P=1.70 \times 10^{-2}$, Supplementary Figures 1a and b, $P=2.00 \times 10^{-5}$ and Supplementary Figure 1c, $P=2.90 \times 10^{-3}$), whereas

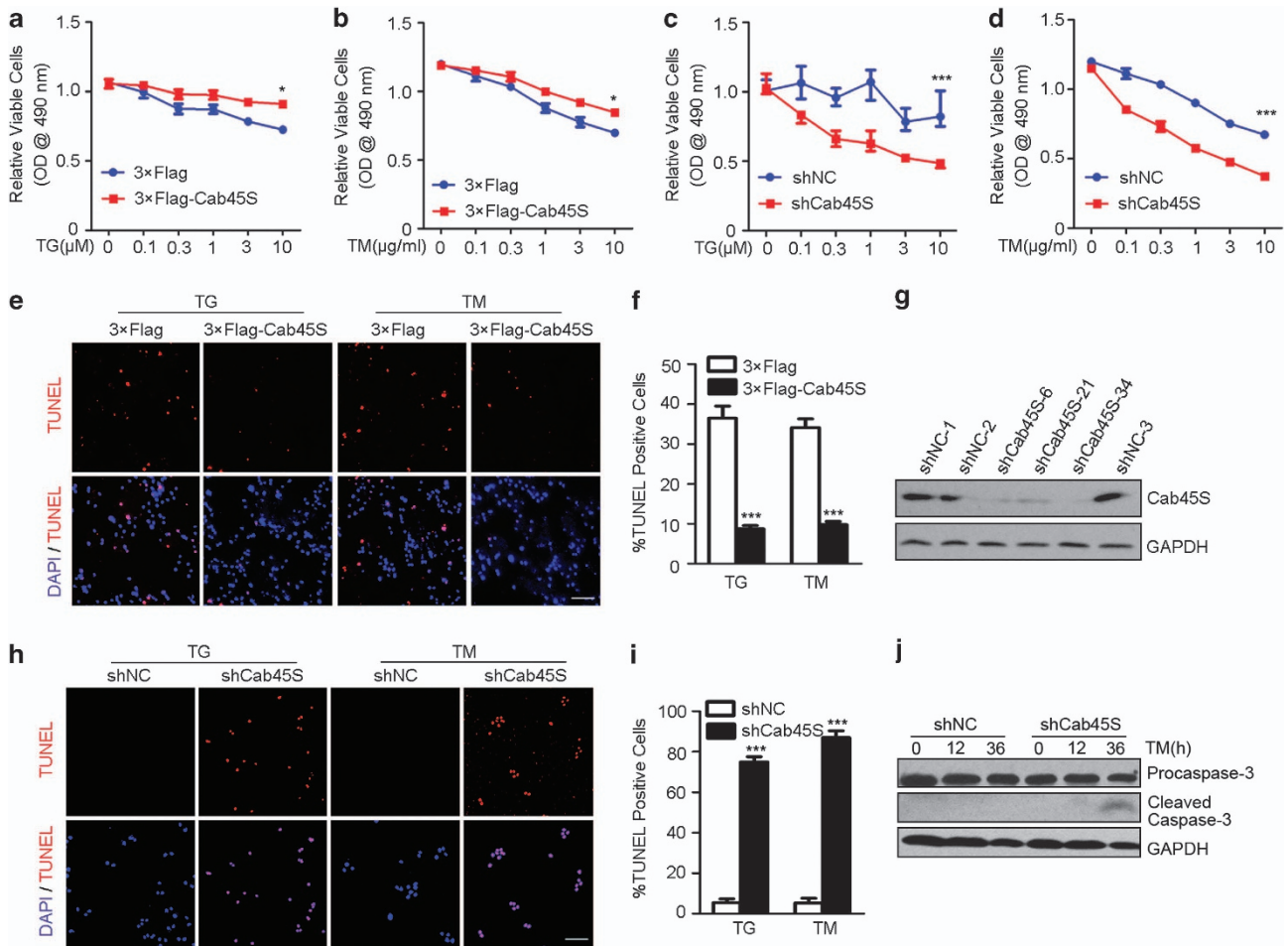


Figure 1 Cab45S promotes cell survival and protects cells from drug-induced apoptosis. **(a and b)** MTS assay of viable HeLa cells overexpressing 3 × Flag or 3 × Flag-Cab45S treated with different TG **(a)** or TM **(b)** concentrations for 48 h ($n=3$). **(c and d)** MTS assay of viable HeLa cells overexpressing scrambled shRNA (shNC) or Cab45S shRNA (shCab45S) treated with different concentrations of TG **(c)** or TM **(d)** for 48 h ($n=3$). **(e)** Representative photomicrographs from TUNEL assay of apoptotic HeLa cells transfected with vectors expressing 3 × Flag and 3 × Flag-Cab45S, treated with TG (2 μM) or TM (2 μg/ml) for 48 h. Scale bar, 100 μm. **(f)** Quantification of TUNEL-positive cells as in **e** ($n=3$; > 100 cells per experiment). **(g)** Western blots of Cab45S from stable HeLa cell lines with Cab45S knockdown. Numbers represent different cell lines. **(h)** Representative photomicrographs from TUNEL assay of apoptotic cells labeled in Cab45S-knockdown HeLa cells treated with TG (2 μM) or TM (2 μg/ml) for 24 h. Scale bar, 100 μm. **(i)** Quantification of TUNEL-positive cells as in **h** ($n=3$; > 100 cells per experiment). **(j)** Western blots of procaspase-3 and cleaved caspase-3 in Cab45S-knockdown HeLa cells after treatment with TM for the indicated times. For **a–d**, data are presented as mean ± S.E.M. * $P<0.05$, *** $P<0.001$, as determined by two-way ANOVA. For **f** and **i**, data are presented as mean ± S.E.M. *** $P<0.001$, determined by unpaired two-tailed Student's *t*-test

depletion of Cab45S rendered the cells less viable in a dose- and time-dependent manner (Figure 1c, $P=2.03 \times 10^{-6}$ and Figure 1d, $P=7.58 \times 10^{-6}$, Supplementary Figures 1d and e, $P=3.61 \times 10^{-2}$ and Supplementary Figure 1f, $P=2.50 \times 10^{-5}$). To further investigate whether Cab45S promotes cell survival by inhibiting apoptosis, we performed terminal deoxynucleotidyl transferase dUTP nick end labeling (TUNEL) assay in TG- or TM-treated HeLa cells, and found that overexpression of $3 \times$ Flag-Cab45S dramatically decreased the number of TUNEL-labeled cells (Figures 1e and f, left, $P=1.26 \times 10^{-4}$, right, $P=3.98 \times 10^{-5}$). Furthermore, we generated stable HeLa cell lines with Cab45S depletion (Figure 1g), in which more cells were labeled as TUNEL positive after TG or TM treatment compared with control cell lines (Figures 1h and i, left, $P=4.58 \times 10^{-7}$, right, $P=9.67 \times 10^{-7}$), and similar results were also obtained in Cab45S-knockdown SW480 and HepG2 cells (Supplementary Figures 1g, h and i, left, $P=3.79 \times 10^{-4}$, right, $P=2.08 \times 10^{-8}$). In addition, a distinct cleaved caspase-3 band appeared in Cab45S-knockdown HeLa cells after treatment with TM for 36 h (Figure 1j), indicating that Cab45S depletion promotes TM-induced apoptosis. Taking these results together, we concluded that Cab45S inhibits ER stress-induced apoptosis.

Cab45S depletion enhances ER stress-induced apoptosis via activation of the IRE1-JNK signaling. To determine by which signaling pathway that Cab45S inhibits ER stress-induced apoptosis, we performed quantitative real-time PCR and measured the transcription levels of UPR-related genes. The results showed that the mRNA level of XBP1s, a spliced form of XBP that is cleaved by IRE1,²⁴ was significantly increased in Cab45S-knockdown HeLa cell lines after 4 h of TM treatment, but ATF4 activation, downstream of PERK,²⁵ was not increased (Figure 2a, $P=5.16 \times 10^{-6}$, and Supplementary Figures 2a and b). ER degradation enhancer, mannosidase alpha-like 1 and ER-localized DnaJ 4/microvascular differentiation gene 1 (ERdj4), the targets of XBP1s,^{26,27} showed patterns similar to XBP1s (Supplementary Figures 2c, $P=1.88 \times 10^{-6}$ and d, $P=3.09 \times 10^{-6}$), whereas CHOP, induced by ATF4,²⁸ showed almost no change (Figure 2b and Supplementary Figure 2e), implying that Cab45S regulates the IRE1- rather than the PERK-mediated pathway after TM treatment.

To verify that Cab45S participated in the IRE1-mediated pathway, we detected phosphorylated IRE1 (p-IRE1), the active form of IRE1, and found that p-IRE1 increased significantly from 6 h after TM treatment in Cab45S-knockdown HeLa cell lines, but decreased in control cell lines (Figures 2b and c, $P_{6h}=2.96 \times 10^{-3}$, $P_{12h}=5.66 \times 10^{-3}$, $P_{24h}=3.16 \times 10^{-4}$). Moreover, we selected efficient shRNAs targeting IRE1 and PERK (Supplementary Figures 2f and g), and used them in the MTS assay. The assay revealed that simultaneous knockdown of IRE1, but not PERK, restored the decreased cell survival caused by Cab45S depletion (Figure 2d, left, $P=1.07 \times 10^{-3}$, right, $P=2.91 \times 10^{-3}$), indicating that IRE1 function as a downstream effector of Cab45S. In addition, TUNEL assay confirmed that simultaneous depletion of IRE1 resulted in a significant decrease of apoptotic cells caused by depletion of Cab45S (Figures 2e

and f, left, $P=5.34 \times 10^{-4}$, right, $P=2.45 \times 10^{-4}$). To further confirm that Cab45S is involved in the IRE1 signaling pathway, we determined the phosphorylation of its downstream effector, phosphorylated JNK (p-JNK), which is crucial for apoptosis.⁸ We found that p-JNK1 in Cab45S-knockdown HeLa cell lines was significantly increased after treatment with TM for 18 h, followed by cleavage of caspase-3, an indicator of apoptosis²⁹ (Figure 2g), whereas sp600125, a JNK inhibitor, prevented cleavage of caspase-3 in Cab45S-knockdown HeLa cell lines 24 h after TM treatment (Figure 2h). This suggests that Cab45S promotes ER stress-induced apoptosis through the IRE1-JNK signaling pathway. Furthermore, we measured the mRNA level of BAX, an important pro-apoptotic regulator associated with IRE1,³⁰ and found that it was significantly upregulated in Cab45S-knockdown HeLa cell lines after 18 h of TM treatment (Figure 2i, $P=3.06 \times 10^{-2}$), implying that BAX may also participate in the apoptotic process. Taken together, these data reveal that the IRE1-JNK signaling pathway serves as a downstream effector of Cab45S to inhibit ER stress-induced apoptosis.

Cab45S interacts with GRP78/BiP. To further investigate how Cab45S functions in the inhibition of ER stress-induced apoptosis, we performed immunoprecipitation assay in HEK293T cells overexpressing $3 \times$ Flag-Cab45S with anti-Flag antibody to screen for Cab45S-interacting proteins. Among the identified potential binding proteins, GRP78/BiP was the most abundant (Figure 3a, Supplementary Table 1). As it is a vital regulator of ER stress,^{31,32} we focused on GRP78/BiP.

Immunoprecipitation assay confirmed that exogenously expressed GRP78/BiP-EGFP specifically interacted with $3 \times$ Flag-Cab45S, but not with other CREC family members $3 \times$ Flag-Cab45G and $3 \times$ Flag-RCN1 (Figure 3b). Furthermore, we co-transfected $3 \times$ Flag-Cab45S and GRP78/BiP-EGFP into HeLa and COS-7 cells, and found that these fusion proteins co-localized in the ER (Supplementary Figure 3). We then constructed GFP-tagged N- and C-terminal truncation mutants of GRP78/BiP and co-transfected them with $3 \times$ Flag-Cab45S into HEK293T cells to map the interaction domain on GRP78/BiP by immunoprecipitation assay. The results showed that the N-terminal nucleotide-binding domain (NBD) of GRP78/BiP was crucial for its interaction with Cab45S (Figures 3c and d); whereas GRP78/BiP interacted with both the N- and C-terminus of Cab45S, yet these interactions were weaker than with the full-length Cab45S (Figures 3e and f), suggesting that the whole structure of Cab45S is necessary for its interaction with GRP78/BiP. To summarize, our results reveal that Cab45S specifically interacts with the NBD of GRP78/BiP in the ER.

Cab45S increases the GRP78/BiP protein level. To determine the effect of Cab45S binding to GRP78/BiP, we first evaluated the GRP78/BiP expression level in PANC-1 cells, which are reported to have increased protein levels of Cab45S in malignant pancreatic secretome.²³ In Cab45S-depleted stable PANC-1 cell lines, the protein level of GRP78/BiP was markedly decreased, but ER chaperones such as PDI and calnexin were not, compared with control cells (Figure 4a). Similar results were also obtained in

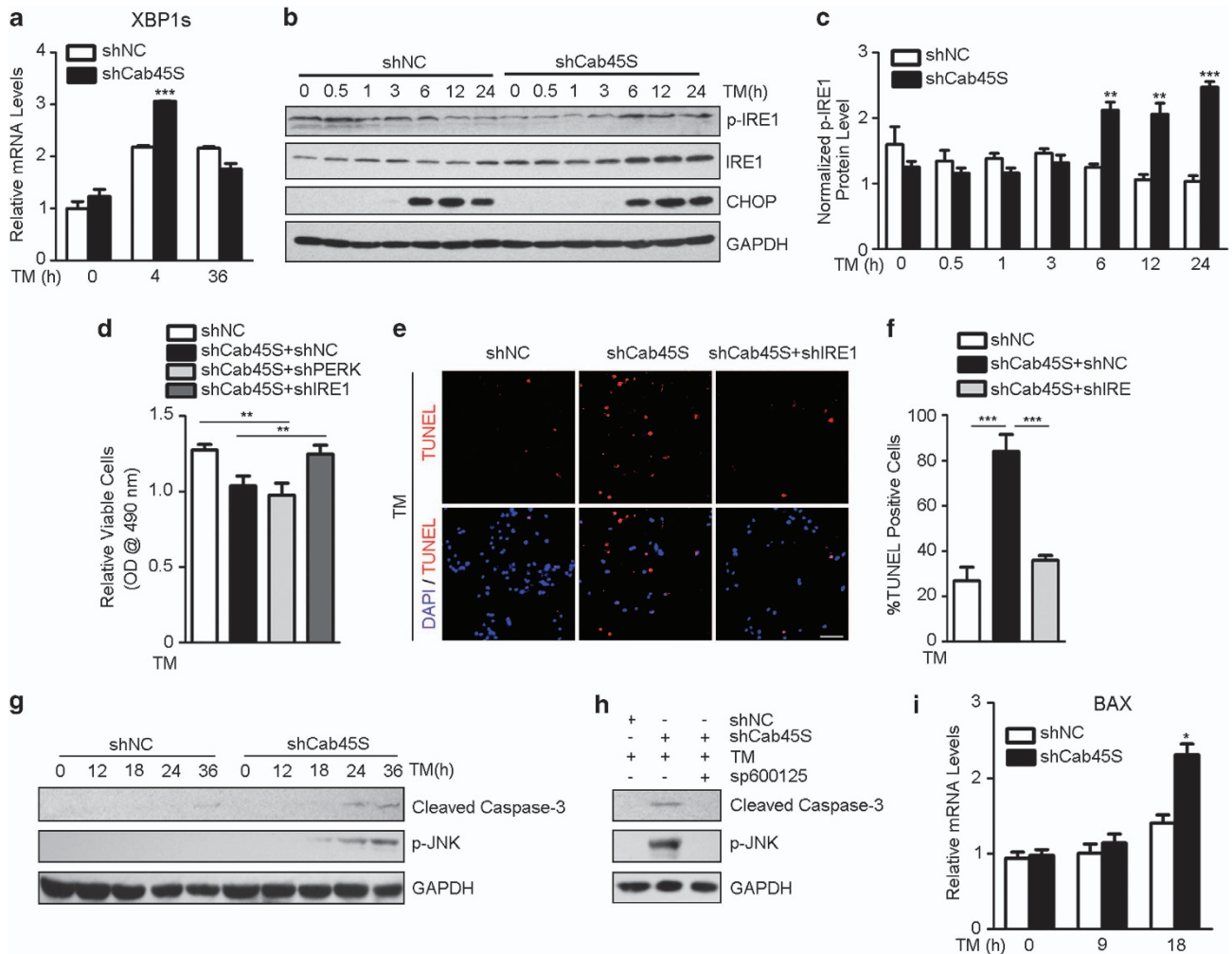


Figure 2 The IRE1-JNK signaling is required for activating ER stress-induced apoptosis in Cab45S-depleted cells. (a) Quantitative real-time PCR of relative mRNA expression levels of XBP1S in control (shNC, scrambled shRNA) and Cab45S-knockdown HeLa cell lines treated with TM (2 μ g/ml) for the indicated periods ($n=3$). (b) Western blots of CHOP, IRE1 and p-IRE1 in control and Cab45S-knockdown HeLa cell lines after treatment with TM (2 μ g/ml) at the indicated time points. (c) Quantification of p-IRE1 in b. GAPDH was used as a loading control. (d) MTS assay of viable HeLa cells transfected with vectors expressing shNC, shCab45S and shNC, shCab45S and shPERK, and shCab45S and shIRE1 with TM (2 μ g/ml) treatment ($n=3$). (e) Representative photomicrographs of apoptotic cells in transfected HeLa cells in which Cab45S or both Cab45S and IRE1 were depleted with TM (2 μ g/ml, 48 h) treatment (TUNEL assay). Scale bar, 100 μ m. (f) Quantification of TUNEL-positive cells as in e ($n=3$; > 100 cells per experiment). (g) Western blots of cleaved caspase-3 and p-JNK in control and Cab45S-knockdown HeLa cell lines after treatment with TM (2 μ g/ml) at the indicated time points. (h) Western blots of cleaved caspase-3 and p-JNK in control and Cab45S-knockdown HeLa cell lines after 24 h treatment with indicated drugs. TM, 2 μ g/ml; sp600125, 20 μ M. (i) Quantitative real-time PCR of relative mRNA expression levels of BAX in control and Cab45S-knockdown HeLa cell lines treated with TM (2 μ g/ml) for the indicated periods ($n=3$). For a, c, d, f and i, data are presented as mean \pm S.E.M. * P <0.05, ** P <0.01, *** P <0.001, as determined by unpaired two-tailed Student's t -test

TM-treated Cab45S-knockdown HeLa cells (Figures 4b and c, left, $P=2.84 \times 10^{-3}$, right, $P=6.05 \times 10^{-3}$). By contrast, we found a strong increase of GRP78/BiP, but not PDI and calnexin, in Cab45S-overexpressing PANC-1 cell lines (Figure 4d, supplementary Figures 4a and b). Intriguingly, we found that unlike the protein level, the GRP78/BiP mRNA level increased in Cab45S-knockdown HeLa cells after 4 h of TM treatment (Figure 4e, $P=1.25 \times 10^{-4}$), indicating that Cab45S directly decreases the GRP78/BiP protein levels. Indeed, rather than affecting GRP78/BiP secretion (Supplementary Figures 4c and d), after 24 h of TM treatment followed by being treated with cycloheximide, a translation inhibitor, knockdown of Cab45S resulted in less remaining GRP78/BiP protein (Figure 4f), suggesting Cab45S depletion

promotes GRP78/BiP degradation. Taken together, Cab45S increases GRP78/BiP protein level by inhibiting its degradation.

Cab45S inhibits ER stress-induced apoptosis via GRP78/BiP. To explore the functional relationship between Cab45S and GRP78/BiP in ER stress-induced apoptosis, we first assessed the cell viability by MTS assay. Overexpression of Cab45S promoted cell survival under TM treatment, yet this effect was disappeared when GRP78/BiP was simultaneously depleted (Figure 5a, $P=4.66 \times 10^{-3}$ and Supplementary Figure 5a), whereas overexpression of GRP78/BiP-EGFP rescued the decreased cell survival caused by Cab45S depletion (Figure 5b, $P=3.43 \times 10^{-3}$

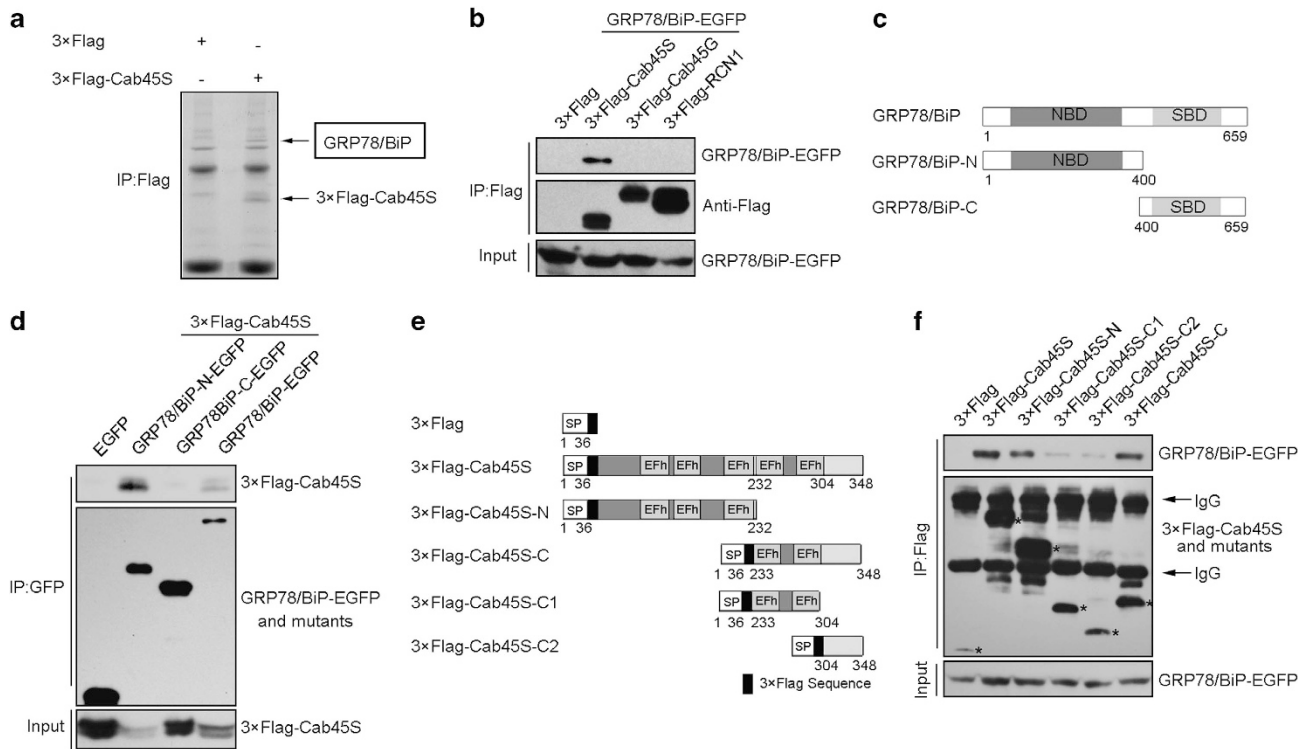


Figure 3 Cab45S interacts with the nucleotide-binding domain (NBD) of GRP78/BiP. (a) Immunoprecipitation assay (IP) with anti-Flag antibody in HEK293T cell lysates expressing 3 × Flag-Cab45S. Immunoprecipitates were subjected to SDS-PAGE and then MS analysis. (b) Extracts of HEK293T cells co-transfected with GRP78/BiP-EGFP and 3 × Flag, 3 × Flag-Cab45S, 3 × Flag-Cab45G or 3 × Flag-RCN1 were immunoprecipitated using anti-Flag antibody. The immunoprecipitates were immunoblotted with anti-Flag or anti-GFP antibody. (c and d) Mapping the domain at which GRP78/BiP interacted with Cab45S. Schematics of GRP78/BiP truncates (c). Extracts of HEK293T cells overexpressing GFP-tagged GRP78/BiP truncates and 3 × Flag-Cab45S were immunoprecipitated with anti-GFP antibody, and the immunoprecipitates were immunoblotted with anti-GFP or anti-Flag antibody (d). SBD, substrate-binding domain. (e and f) Mapping the domain of Cab45S, which interacted with GRP78/BiP. Schematics of Cab45S truncates (e). Extracts of HEK293T cells overexpressing 3 × Flag-tagged Cab45S truncates and GRP78/BiP-EGFP were immunoprecipitated with anti-Flag antibody, and the immunoprecipitates were immunoblotted with anti-GFP and anti-Flag antibodies (f). Asterisks indicate 3 × Flag-tagged Cab45S truncates immunoprecipitated by anti-Flag antibody. SP, signal peptide; EFh, EF-hand

and Supplementary Figure 5b). This suggests that Cab45S, as an upstream regulator of GRP78/BiP, promotes cell survival during ER stress. Next, to further determine whether Cab45S protects cells from ER stress-induced apoptosis via GRP78/BiP, we performed TUNEL assay. Under TM treatment, overexpression of Cab45S showed decreased labeling of apoptotic cells, and this phenotype disappeared when GRP78/BiP was simultaneously depleted (Figures 5c and d, left, $P=2.9 \times 10^{-3}$, right, $P=4.5 \times 10^{-4}$). On the other hand, knockdown of Cab45S resulted in more labeling of apoptotic cells, whereas simultaneous overexpression of GRP78/BiP-EGFP decreased the number of apoptotic cells to the level in control cells (Figures 5e and f, left, $P=5.34 \times 10^{-4}$, right, $P=1.5 \times 10^{-4}$), indicating that Cab45S inhibits ER stress-induced apoptosis via GRP78/BiP.

Cab45S inhibits ER stress-induced IRE1 activation mediated by GRP78/BiP. To test whether GRP78/BiP was also involved in the inhibition of ER stress-induced IRE1 activation triggered by Cab45S, we measured the IRE1 phosphorylation level in HeLa cells. The results showed that after TM treatment, overexpression of Cab45S suppressed IRE1 phosphorylation, and this phenotype was reversed when GRP78/BiP was simultaneously depleted (Figures 6a

and b, left, $P=2.45 \times 10^{-6}$, right, $P=5.66 \times 10^{-3}$). Meanwhile, knockdown of Cab45S promoted IRE1 phosphorylation under TM treatment, whereas overexpression of GRP78/BiP-EGFP decreased IRE1 phosphorylation to normal level (Figures 6c and d, left, $P=1.05 \times 10^{-5}$, right, $P=2.38 \times 10^{-4}$). Furthermore, after 24 h of TM treatment, depletion of Cab45S resulted in less GRP78/BiP-EGFP co-immunoprecipitation with 3 × Flag-IRE1 in HEK293T cells (Figure 6e). Together, these results suggest that Cab45S inhibits ER stress-induced IRE1 activation via GRP78/BiP, and stabilizes the interaction between GRP78/BiP and IRE1.

Discussion

Cab45S has been previously reported to be a secreted protein, but its function is largely obscure.²³ In the present study, we provide evidence that Cab45S co-localizes and interacts with GRP78/BiP in the ER. Cab45S increases the GRP78/BiP protein level and prevents GRP78/BiP disassociating from IRE1 during ER stress condition to suppress the IRE1-JNK signaling pathway, and inhibits apoptosis (Figure 6f).

GRP78/BiP, a chaperone predominantly in the ER lumen, interacts with unfolded proteins through its C-terminal

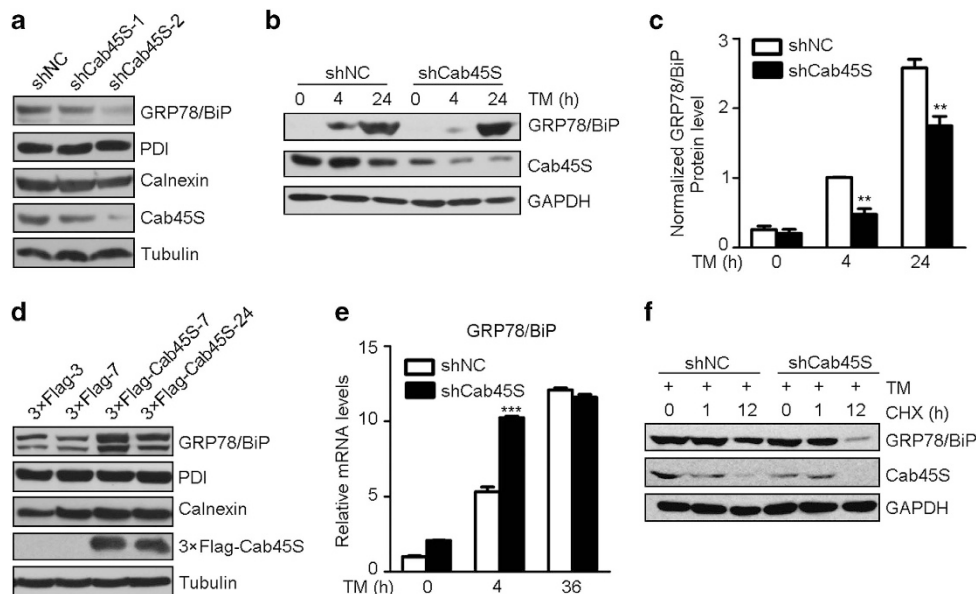


Figure 4 Cab45S increases the GRP78/BiP protein level. (a and d) Western blots of GRP78/BiP and two other ER molecular chaperones, PDI and calnexin, in stable Cab45S-knockdown (a) or Cab45S-overexpressed (d) PANC-1 cell lines. Numbers represent different cell lines. (b and c) Western blots (b) and quantification (c) of GRP78/BiP in Cab45S-knockdown and control (shNC, scrambled shRNA) HeLa cells treated with TM (2 μ g/ml) for the indicated periods. GAPDH was used as a loading control. (e) Quantitative real-time PCR of the relative GRP78/BiP mRNA expression levels in Cab45S-knockdown and control HeLa cells treated with TM for the indicated times ($n = 3$). (f) Western blots of GRP78/BiP in Cab45S-knockdown and control HeLa cells treated with TM (2 μ g/ml, 4 h) followed by cycloheximide (Chx; 100 μ M) for the indicated periods. For c and e, data are presented as mean \pm S.E.M. ** $P < 0.01$, *** $P < 0.001$, as determined by unpaired two-tailed Student's *t*-test

substrate-binding domain, which is tightly regulated by a conformational change that depends on ATP occupation of its NBD.³³ Our results show that Cab45S binds to the NBD of GRP78/BiP, and this binding is specific for Cab45S but not other members of the CREC family such as Cab45G and RCN1. However, both the N- and C-terminus of Cab45S are involved in the interaction with GRP78/BiP, suggesting that the structural integrity of Cab45S is essential for this interaction, and the regulation of Cab45S binding to GRP78/BiP is complex. Previous reports suggested that some proteins, including BAP/Sil1 and ERdj4, also bind to the NBD of GRP78/BiP as co-chaperones to regulate its function. BAP/Sil1, the first nucleotide exchange factor identified in the mammalian ER,³⁴ binds to GRP78/BiP and this leads to a higher substrate-releasing ratio.³⁵ ERdj4 stabilizes the substrate binding of GRP78/BiP by inhibiting the connection between the NBD and the substrate-binding domain.^{36,37} Thus, the NBD is crucial for the regulation of substrate binding by GRP78/BiP. However, at this stage, we still do not know the detailed structural basis of this process, and the mechanism underlying modulation of the NBD and substrate binding of GRP78/BiP by Cab45S also deserves further research.

In the unstressed ER lumen, GRP78/BiP binds to PERK, IRE1 and activating transcription factor 6 to inhibit their oligomerization and phosphorylation, whereas during ER stress, GRP78/BiP releases these receptors leading to their activation.³² Our data show that depletion of Cab45S increases the activation of IRE1, but not PERK. Considering that Cab45S may regulate substrate binding by GRP78/BiP and the substrate-chaperone manner of interaction between IRE1 and GRP78/BiP, one possible mechanism by which Cab45S inhibits IRE1 activity is that Cab45S stabilizes the

interaction between GRP78/BiP and IRE1 by increasing substrate-binding ability of GRP78/BiP, similar to ERdj4.³⁶ Yet there may be other mechanisms by which Cab45S inhibits IRE1 activity. For example, in Cab45S-depleted cells during ER stress, a decrease of GRP78/BiP protein level and an increase of the BAX mRNA level might account for the regulation of IRE1 activation. But the mechanism underlying the selectivity for IRE1 activation remains unknown.

IRE1 has both kinase and endonuclease activity. During ER stress, activated IRE1 splices XBP1 mRNA to the mature form XBP1s, which mainly has a protective role by initiating a series of genes involved in restoring protein folding or ER-associated protein degradation, whereas prolonged ER stress increases IRE1 kinase activity, which increases JNK phosphorylation that is linked to apoptosis.⁶ However, a previous report suggested that these two activities of IRE1 are relatively independent.³⁸ Indeed, our data show that in the prolonged ER stress, Cab45S depletion leads to slightly less XBP1s, in contrast to the increased JNK1 phosphorylation, suggesting that at this time, the increased IRE1 phosphorylation mainly contributes to its kinase activity in ER stress-induced apoptosis.

In many tumors, GRP78/BiP is highly expressed and is vital for tumor cell survival.¹³ Recent studies have shown that during severe ER stress, several proteins such as RRBP1 and clusterin prevent apoptosis in a chaperone-dependent manner in cancer cell lines. RRBP1 interacts with GRP78/BiP and enhances its levels to reduce apoptosis in lung cancer,³⁹ whereas clusterin has a similar effect in the hepatocellular carcinoma.⁴⁰ However, the molecular mechanisms underlying how these proteins increase GRP78/BiP level are obscure. Consistently, we find that Cab45S interacts with

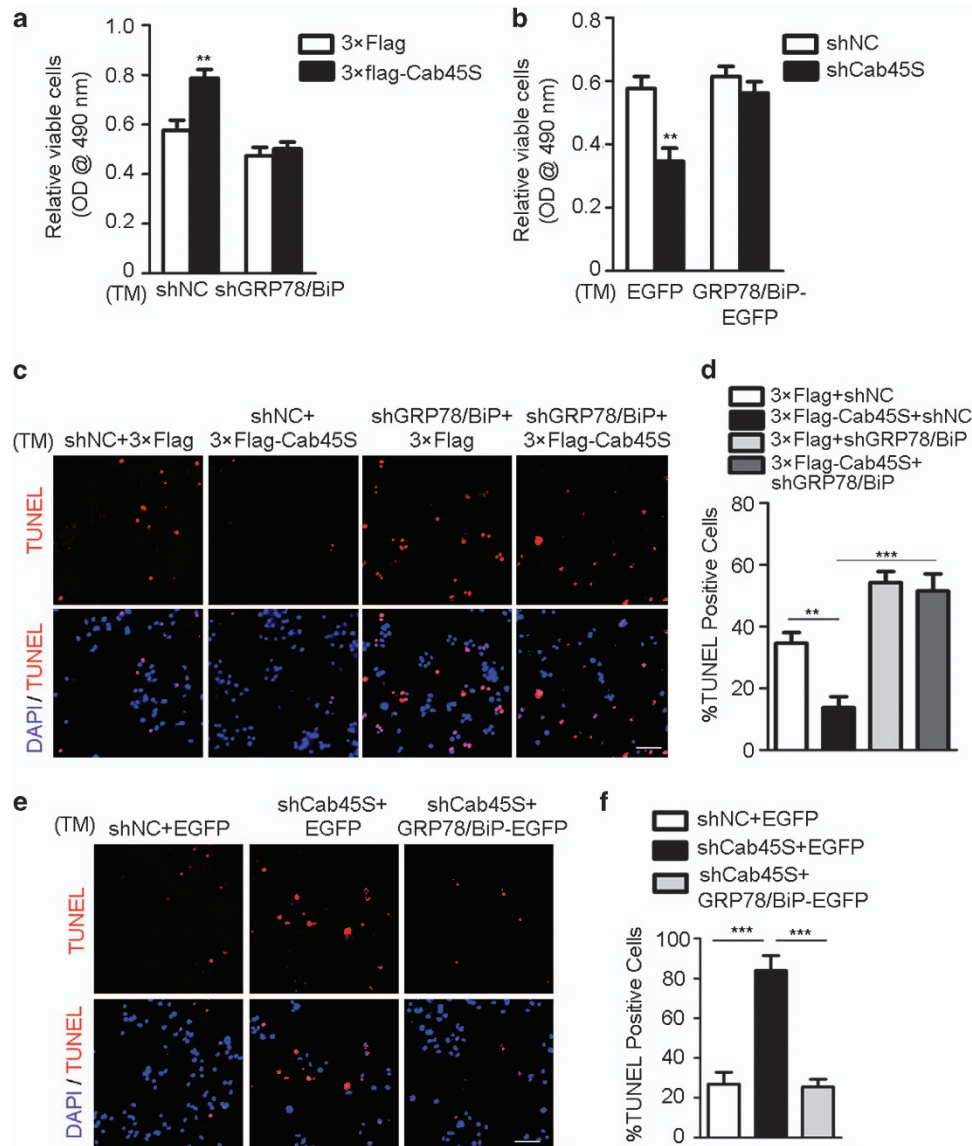


Figure 5 Cab45S inhibits ER stress-induced apoptosis via GRP78/BiP. (a) MTS assay of viable HeLa cells transfected with vectors expressing 3 × Flag and shNC (scrambled shRNA), 3 × Flag-Cab45S and shNC, 3 × Flag and shGRP78/BiP, or 3 × Flag-Cab45S and shGRP78/BiP treated with TM (2 μg/ml, 48 h; n = 3). (b) MTS assay of viable HeLa cells transfected with vectors expressing shNC and EGFP, shCab45S and EGFP, shNC and GRP78/BiP-EGFP, or shCab45S and GRP78/BiP-EGFP treated with TM (2 μg/ml, 48 h; n = 3). (c) Representative photomicrographs from TUNEL assay of apoptotic HeLa cells transfected with vectors expressing 3 × Flag and shNC, 3 × Flag-Cab45S and shNC, 3 × Flag and shGRP78/BiP, or 3 × Flag-Cab45S and shGRP78/BiP treated with TM (2 μg/ml, 48 h). Scale bar, 100 μm. (d) Quantification of TUNEL-positive cells as in c (n = 3; > 100 cells per experiment). (e) Representative photomicrographs from TUNEL assay of apoptotic HeLa cells transfected with vectors expressing shNC and EGFP, shCab45S and EGFP, or shCab45S and GRP78/BiP-EGFP treated with TM (2 μg/ml, 48 h). Scale bar, 100 μm. (f) Quantification of TUNEL-positive cells as in e (n = 3; > 100 cells per experiment). For a, b, d and f, data are presented as mean ± S.E.M. **P < 0.01, ***P < 0.001, as determined by unpaired two-tailed Student's t-test

GRP78/BiP, and Cab45S depletion promotes ER stress-induced apoptosis by decreasing the GRP78/BiP protein level. But in contrast with its protein level, the mRNA level of GRP78/BiP increases, which may be due to the enhanced splicing of XBP1. We moved a step forward by demonstrating that Cab45S stabilizes GRP78/BiP protein to prevent degradation but not secretion, thus attenuating IRE1-mediated signaling to protect cells from ER stress-induced apoptosis. But whether this effect is due to the interaction between them or requires other proteins for assistance needs further

investigation. As GRP78/BiP is a promising target in cancer therapy,⁴¹ elucidation of the relationship between Cab45S and GRP78/BiP may thus lead to novel clinical therapies for cancer.

Materials and Methods

Vector construction. Cab45S/G and RCN1 were cloned from HeLa cell cDNA and inserted into the pcDNA3.1+ vector (Invitrogen, Carlsbad, CA, USA) with an EGFP or 3 × Flag tag immediately after their signal peptides. GRP78/BiP was also cloned from HeLa cell cDNA and inserted into the pEGFP-N3 vector

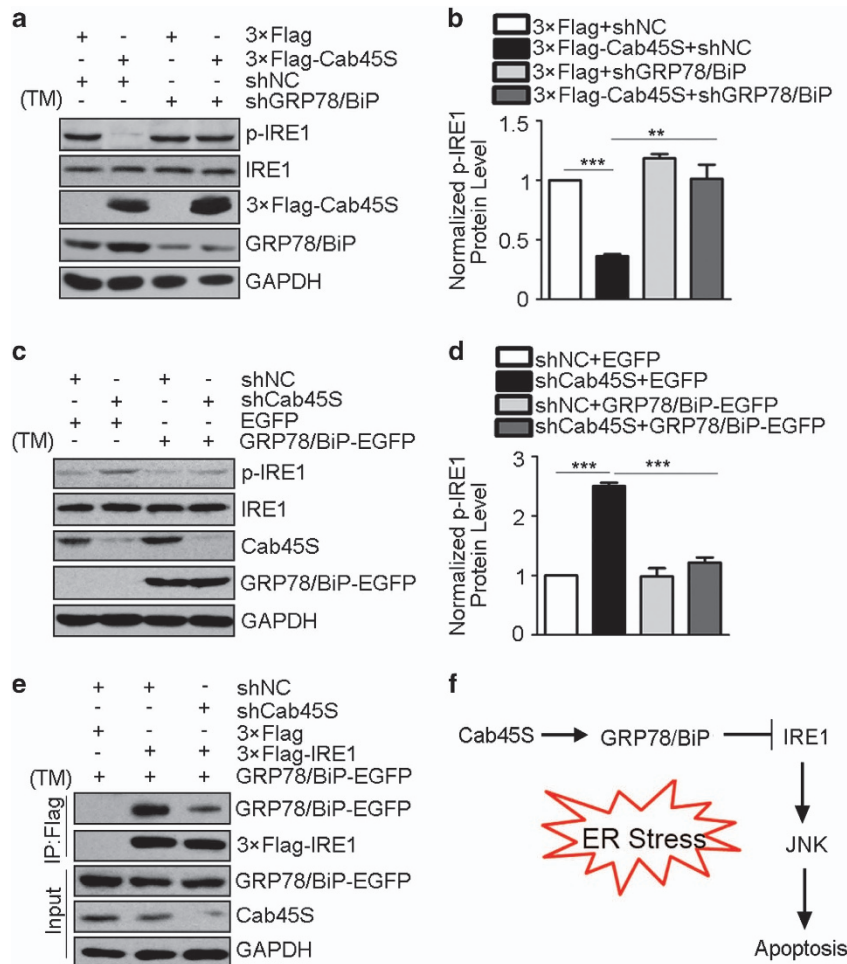


Figure 6 Cab45S inhibits IRE1 activation via GRP78/BiP. (a and b) Western blots (a) and quantification (b) of p-IRE1 in HeLa cells transfected with vectors expressing 3 × Flag and shNC (scrambled shRNA), 3 × Flag-Cab45S and shNC, 3 × Flag and shGRP78/BiP, or 3 × Flag-Cab45S and shGRP78/BiP after TM treatment (2 μg/ml, 48 h). GAPDH was used as a loading control. (c and d) Western blots (c) and quantification (d) of p-IRE1 in HeLa cells expressing shNC and EGFP, shCab45S and EGFP, shNC and GRP78/BiP-EGFP, or shCab45S and GRP78/BiP-EGFP after TM treatment (2 μg/ml, 48 h). GAPDH was used as a loading control. (e) Extracts of HEK293T cells overexpressing the indicated vectors treated with TM (1 μg/ml, 24 h) were immunoprecipitated with anti-Flag antibody. The immunoprecipitates were immunoblotted with anti-Flag, anti-EGFP or anti-Cab45S antibody. (f) Working model of the mechanism by which Cab45S controls ER stress-induced apoptosis. Cab45S interacts with the NBD of GRP78/BiP, which prevents its disassociation from IRE1 and increases the protein level of GRP78/BiP. These effects lead to inhibition of the IRE1-JNK pathway and ER stress-induced apoptosis. For b and d, data are presented as mean ± S.E.M. ***P* < 0.01, ****P* < 0.001, as determined by unpaired two-tailed Student's *t*-test

(Clontech Laboratories, Mountain View, CA, USA). The truncations of Cab45S and GRP78/BiP were constructed based on the 3 × Flag-Cab45S and GRP78/BiP-EGFP vectors.

RNAi. The followings were the shRNA sequences used in the experiments: Cab45S sh1: 5'-TCAAGTACAGCGAGTTCT-3', sh2: 5'-GGAGGAAGCT GATGGTCA-3' (Sigma, St. Louis, MO, USA); PERK sh4: 5'-GAAACTCTACCA GCCTCTA-3', sh5: 5'-GAAACAGCTATTCTCATAAAG-3' (Sigma); IRE1 sh3: 5'-GAGAAGATGATTGCGATGGAT-3', sh4: 5'-GAAACTCTACCAGCCTCTA-3' (Sigma); GRP78/BiP sh1: 5'-ACAAGAAGGAGGACGTGGCA-3', sh2: 5'-GC TAATTGAGACCACAGGCTT-3' (Sigma).

Cell culture. HeLa, HEK293T, SW480, HepG2 and COS-7 cells were cultured in DMEM (GIBCO BRL, Grand Island, NY, USA), and PANC-1 cells were cultured in RPMI 1640 (GIBCO), which were supplemented with 10% FBS (HyClone, Logan, UT, USA) at 37 °C with 5% CO₂.

Reagents and antibodies. The primary antibodies were anti-BrdU (MBL, Nagoya, Japan), anti-GFP (MBL), anti-Flag (Sigma), anti-tubulin (Sigma),

anti-ATF4 (GeneTex, San Antonio, TX, USA) and anti-PARP, anti-calnexin, anti-PDI, anti-p-JNK, anti-caspase-3, anti-PERK, anti-IRE1, anti-GAPDH, anti-pIRE1 and anti-GRP78/BiP from Cell Signaling Technologies (Danvers, MA, USA). Anti-Cab45S antibody was raised against the peptide in the C-terminal domain (305–348 aa) different from Cab45G. The secondary antibodies used were as follows: HRP-conjugated and AlexaFluor 488-/568-conjugated goat anti-mouse/rabbit IgG antibodies (Invitrogen) for western blotting and immunofluorescence, respectively. The drugs used were TG (Sigma), TM (Sigma), sp600125 (Cell Signaling Technologies), cycloheximide (Sigma).

Stable cell line generation. HeLa cells transfected with the plasmids were incubated with puromycin (2 μg/ml) for selection. Single clones were selected and cultured in the presence of puromycin for 2 weeks. Cell lines were then subjected to western blot analysis.

Transfection and immunofluorescence. Cells were grown to 50% confluence and then transfected with PEI. After transfection for 5 h, the medium was replaced, and cultured cells with or without drugs for the indicated times were used for subsequent study.

For immunofluorescence, cells were cultured on glass slides, fixed with 4% PFA for 0.5 h, and then permeabilized with 0.15% Triton X-100, washed three times with PBS, blocked with BSA and exposed to the primary antibody overnight at 4 °C. After rinsing the cells five times with PBS, the samples were exposed to the secondary antibody for 1 h at room temperature, and then washed five times, and used for confocal microscopy (Leica, Solms, Germany).

Immunoprecipitation, mass spectrometry and western blot.

Thirty-six hours after transient transfection, HEK293T cells were lysed on ice in immunoprecipitation buffer (50 mM Tris, 150 mM NaCl, 1% Triton X-100, 1 mM DTT, 2 mM CaCl₂, pH 7.4) with a protease inhibitor cocktail (Roche, Basel, Switzerland). One-tenth of the cell lysates were prepared as input samples, and the rest were pre-cleared with Protein A/G Sepharose beads (GE Healthcare, Uppsala, Sweden) for 0.5 h. Then the supernatant was incubated with primary antibody at 4 °C overnight, after which the beads were added to the system and incubated for 2 h. Then, the beads were rinsed three times in the immunoprecipitation buffer and prepared as immunoprecipitation samples. The samples were separated by SDS-PAGE, followed by western blotting or mass spectrometry (Finnigan, San Diego, CA, USA).

MTS assay. Cells at 5×10^3 per well were seeded in 96-well plates, treated as indicated for 2 or 3 days after transfection, and then assayed using an MTS kit (Promega, Madison, WI, USA). Before measurement, 20 μ l MTS reagent was added into each well. After 1–2 h incubation, viable cells were measured as the absorbance at 490 nm. Each experiment was repeated eight times.

TUNEL assay. HeLa cells on glass slides were transfected, treated with drugs for the indicated times, and subjected to TUNEL labeling according to the recommended procedures (*In Situ* Cell Death Detection kit, TMR red; Roche). After fixation, the cells were permeabilized with 0.1% Triton-X 100 and 0.1% sodium citrate on ice for 2 min. Then they were washed twice, incubated with TUNEL reaction mixture at 37 °C in darkness for 1 h and examined under a fluorescence microscope (Olympus, Tokyo, Japan) as previously described.⁴²

Quantitative real-time PCR. The mRNA was extracted from HeLa cells to synthesize cDNA using the GoScript Reverse Transcription System (Promega). SYBR Green PCR Master Mix (Applied Biosystems, Foster City, CA, USA) was used to perform quantitative real-time PCR in an ABI 7300 Detection System (Applied Biosystems) as previously described.^{43,44} The primer sequences were listed in Supplementary Materials (Supplementary Table 2). All reactions were conducted in triplicate.

Data analysis. All experiments were repeated at least three times. Data analysis was performed with GraphPad Prism 5 software (GraphPad Software, San Diego, CA, USA) using the unpaired two-tailed Student's *t*-test.

Conflict of Interest

The authors declare no conflict of interest.

Acknowledgements. We thank Professor IC Bruce (Zhejiang University) for revising the manuscript, Professor Albert Yu (Peking University) for kindly providing p-JNK antibody and JNK inhibitor (sp600125), and Professor Weiguo Zhu (Peking University) for SW480 cell line. This work was supported by the National Natural Science Foundation of China (31271424) and the Major State Basic Research Development Program of China (973 Program; 2010CB833705).

1. Anelli T, Sitta R. Protein quality control in the early secretory pathway. *EMBO J* 2008; **27**: 315–327.
2. Pizzo P, Pozzan T. Mitochondria-endoplasmic reticulum choreography: structure and signaling dynamics. *Trends Cell Biol* 2007; **17**: 511–517.
3. Kim I, Xu W, Reed JC. Cell death and endoplasmic reticulum stress: disease relevance and therapeutic opportunities. *Nat Rev Drug Discov* 2008; **7**: 1013–1030.
4. Ron D, Walter P. Signal integration in the endoplasmic reticulum unfolded protein response. *Nat Rev Mol Cell Biol* 2007; **8**: 519–529.
5. Hetz C. The unfolded protein response: controlling cell fate decisions under ER stress and beyond. *Nat Rev Mol Cell Biol* 2012; **13**: 89–102.
6. Tabas I, Ron D. Integrating the mechanisms of apoptosis induced by endoplasmic reticulum stress. *Nat Cell Biol* 2011; **13**: 184–190.

7. Shen X, Ellis RE, Lee K, Liu CY, Yang K, Solomon A *et al*. Complementary signaling pathways regulate the unfolded protein response and are required for *C. elegans* development. *Cell* 2001; **107**: 893–903.
8. Urano F, Wang X, Bertolotti A, Zhang Y, Chung P, Harding HP *et al*. Coupling of stress in the ER to activation of JNK protein kinases by transmembrane protein kinase IRE1. *Science* 2000; **287**: 664–666.
9. Nishitoh H, Matsuzawa A, Tobiume K, Saegusa K, Takeda K, Inoue K *et al*. ASK1 is essential for endoplasmic reticulum stress-induced neuronal cell death triggered by expanded polyglutamine repeats. *Genes Dev* 2002; **16**: 1345–1355.
10. Upton JP, Wang L, Han D, Wang ES, Huskey NE, Lim L *et al*. IRE1 α cleaves select microRNAs during ER stress to derepress translation of proapoptotic Caspase-2. *Science* 2012; **338**: 818–822.
11. Munro S, Pelham HR. An Hsp70-like protein in the ER: identity with the 78 kd glucose-regulated protein and immunoglobulin heavy chain binding protein. *Cell* 1986; **46**: 291–300.
12. Lee AS. Mammalian stress response: induction of the glucose-regulated protein family. *Curr Opin Cell Biol* 1992; **4**: 267–273.
13. Dudek J, Benedix J, Cappel S, Greiner M, Jalal C, Muller L *et al*. Functions and pathologies of BiP and its interaction partners. *Cell Mol Life Sci* 2009; **66**: 1556–1569.
14. Li J, Lee AS. Stress induction of GRP78/BiP and its role in cancer. *Curr Mol Med* 2006; **6**: 45–54.
15. Fu Y, Lee AS. Glucose regulated proteins in cancer progression, drug resistance and immunotherapy. *Cancer Biol Ther* 2006; **5**: 741–744.
16. Fu Y, Li J, Lee AS. GRP78/BiP inhibits endoplasmic reticulum BIK and protects human breast cancer cells against estrogen starvation-induced apoptosis. *Cancer Res* 2007; **67**: 3734–3740.
17. Hayashi T, Su TP. Sigma-1 receptor chaperones at the ER-mitochondrion interface regulate Ca(2+) signaling and cell survival. *Cell* 2007; **131**: 596–610.
18. Burikhanov R, Zhao Y, Goswami A, Qiu S, Schwarze SR, Rangnekar VM. The tumor suppressor Par-4 activates an extrinsic pathway for apoptosis. *Cell* 2009; **138**: 377–388.
19. Shani G, Fischer WH, Justice NJ, Kelber JA, Vale W, Gray PC. GRP78 and Cripto form a complex at the cell surface and collaborate to inhibit transforming growth factor beta signaling and enhance cell growth. *Mol Cell Biol* 2008; **28**: 666–677.
20. Kelber JA, Panopoulos AD, Shani G, Booker EC, Belmonte JC, Vale WW *et al*. Blockade of Cripto binding to cell surface GRP78 inhibits oncogenic Cripto signaling via MAPK/PI3K and Smad2/3 pathways. *Oncogene* 2009; **28**: 2324–2336.
21. Honore B. The rapidly expanding CREC protein family: members, localization, function, and role in disease. *Bioessays* 2009; **31**: 262–277.
22. Lam PP, Hyvarinen K, Kauppi M, Cosen-Binker L, Laitinen S, Keranen S *et al*. A cytosolic splice variant of Cab45 interacts with Munc18b and impacts on amylase secretion by pancreatic acini. *Mol Biol Cell* 2007; **18**: 2473–2480.
23. Gronborg M, Kristiansen TZ, Iwahori A, Chang R, Reddy R, Sato N *et al*. Biomarker discovery from pancreatic cancer secretome using a differential proteomic approach. *Mol Cell Proteomics* 2006; **5**: 157–171.
24. Yoshida H, Matsui T, Yamamoto A, Okada T, Mori K. XBP1 mRNA is induced by ATF6 and spliced by IRE1 in response to ER stress to produce a highly active transcription factor. *Cell* 2001; **107**: 881–891.
25. Harding HP, Novoa I, Zhang Y, Zeng H, Wek R, Schapira M *et al*. Regulated translation initiation controls stress-induced gene expression in mammalian cells. *Mol Cell* 2000; **6**: 1099–1108.
26. Kanemoto S, Kondo S, Ogata M, Murakami T, Urano F, Imaizumi K. XBP1 activates the transcription of its target genes via an ACGT core sequence under ER stress. *Biochem Biophys Res Commun* 2005; **331**: 1146–1153.
27. Yu CY, Hsu YW, Liao CL, Lin YL. Flavivirus infection activates the XBP1 pathway of the unfolded protein response to cope with endoplasmic reticulum stress. *J Virol* 2006; **80**: 11868–11880.
28. Outinen PA, Sood SK, Pfeifer SI, Pamidi S, Podor TJ, Li J *et al*. Homocysteine-induced endoplasmic reticulum stress and growth arrest leads to specific changes in gene expression in human vascular endothelial cells. *Blood* 1999; **94**: 959–967.
29. Skov S, Klausen P, Claesson MH. Ligation of major histocompatibility complex (MHC) class I molecules on human T cells induces cell death through PI-3 kinase-induced c-Jun NH2-terminal kinase activity: a novel apoptotic pathway distinct from Fas-induced apoptosis. *J Cell Biol* 1997; **139**: 1523–1531.
30. Hetz C, Bernasconi P, Fisher J, Lee AH, Bassik MC, Antonsson B *et al*. Proapoptotic BAX and BAK modulate the unfolded protein response by a direct interaction with IRE1 α . *Science* 2006; **312**: 572–576.
31. Shen J, Chen X, Hendershot L, Prywes R. ER stress regulation of ATF6 localization by dissociation of BiP/GRP78 binding and unmasking of Golgi localization signals. *Dev Cell* 2002; **3**: 99–111.
32. Bertolotti A, Zhang Y, Hendershot LM, Harding HP, Ron D. Dynamic interaction of BiP and ER stress transducers in the unfolded-protein response. *Nat Cell Biol* 2000; **2**: 326–332.
33. Mayer MP, Bukau B. Hsp70 chaperones: cellular functions and molecular mechanism. *Cell Mol Life Sci* 2005; **62**: 670–684.
34. Chung KT, Shen Y, Hendershot LM. BAP, a mammalian BiP-associated protein, is a nucleotide exchange factor that regulates the ATPase activity of BiP. *J Biol Chem* 2002; **277**: 47557–47563.

35. Awe K, Lambert C, Prange R. Mammalian BiP controls posttranslational ER translocation of the hepatitis B virus large envelope protein. *FEBS Lett* 2008; **582**: 3179–3184.
36. Shen Y, Meunier L, Hendershot LM. Identification and characterization of a novel endoplasmic reticulum (ER) DnaJ homologue, which stimulates ATPase activity of BiP in vitro and is induced by ER stress. *J Biol Chem* 2002; **277**: 15947–15956.
37. Awad W, Estrada I, Shen Y, Hendershot LM. BiP mutants that are unable to interact with endoplasmic reticulum DnaJ proteins provide insights into interdomain interactions in BiP. *Proc Natl Acad Sci USA* 2008; **105**: 1164–1169.
38. Jurczak MJ, Lee AH, Jomayvaz FR, Lee HY, Birkenfeld AL, Guigni BA *et al*. Dissociation of inositol-requiring enzyme (IRE1 α)-mediated c-Jun N-terminal kinase activation from hepatic insulin resistance in conditional X-box-binding protein-1 (XBP1) knock-out mice. *J Biol Chem* 2012; **287**: 2558–2567.
39. Tsai HY, Yang YF, Wu AT, Yang CJ, Liu YP, Jan YH *et al*. Endoplasmic reticulum ribosome-binding protein 1 (RRBP1) overexpression is frequently found in lung cancer patients and alleviates intracellular stress-induced apoptosis through the enhancement of GRP78. *Oncogene* 2013; **32**: 4921–4931.
40. Wang C, Jiang K, Gao D, Kang X, Sun C, Zhang Q *et al*. Clusterin protects hepatocellular carcinoma cells from endoplasmic reticulum stress induced apoptosis through GRP78. *PLoS One* 2013; **8**: e55981.
41. Zhang LH, Zhang X. Roles of GRP78 in physiology and cancer. *J Cell Biochem* 2010; **110**: 1299–1305.
42. He R, Huang N, Bao Y, Zhou H, Teng J, Chen J. LRRC45 is a centrosome linker component required for centrosome cohesion. *Cell Rep* 2013; **4**: 1100–1107.
43. Feng H, Chen L, Wang Q, Shen B, Liu L, Zheng P *et al*. Calumenin-15 facilitates filopodia formation by promoting TGF- β superfamily cytokine GDF-15 transcription. *Cell Death Dis* 2013; **4**: e870.
44. Wang Q, Feng H, Zheng P, Shen B, Chen L, Liu L *et al*. The intracellular transport and secretion of calumenin-1/2 in living cells. *PLoS One* 2012; **7**: e35344.



Cell Death and Disease is an open-access journal published by Nature Publishing Group. This work is licensed under a Creative Commons Attribution-NonCommercial-NoDerivs 3.0 Unported License. The images or other third party material in this article are included in the article's Creative Commons license, unless indicated otherwise in the credit line; if the material is not included under the Creative Commons license, users will need to obtain permission from the license holder to reproduce the material. To view a copy of this license, visit <http://creativecommons.org/licenses/by-nc-nd/3.0/>

Supplementary Information accompanies this paper on Cell Death and Disease website (<http://www.nature.com/cddis>)